

Dynamic circuit motifs underlying rhythmic gain control, gating and integration

Thilo Womelsdorf^{1,2}, Taufik A Valiante^{3,4}, Ned T Sahin^{5,6}, Kai J Miller^{7,8} & Paul Tiesinga⁹

Brain circuitry processes information by rapidly and selectively engaging functional neuronal networks. The dynamic formation of networks is often evident in rhythmically synchronized neuronal activity and tightly correlates with perceptual, cognitive and motor performances. But how synchronized neuronal activity contributes to network formation and how it relates to the computation of behaviorally relevant information has remained difficult to discern. Here we structure recent empirical advances that link synchronized activity to the activation of so-called dynamic circuit motifs. These motifs explicitly relate (1) synaptic and cellular properties of circuits to (2) identified timescales of rhythmic activation and to (3) canonical circuit computations implemented by rhythmically synchronized circuits. We survey the ubiquitous evidence of specific cell and circuit properties underlying synchronized activity across theta, alpha, beta and gamma frequency bands and show that their activation likely implements gain control, context-dependent gating and state-specific integration of synaptic inputs. This evidence gives rise to the dynamic circuit motifs hypothesis of synchronized activation states, with its core assertion that activation states are linked to uniquely identifiable local circuit structures that are recruited during the formation of functional networks to perform specific computational operations.

Functional brain networks are characterized by temporally correlated activity across multiple, distributed brain circuits. Such temporal correlation is measured as synchronized activation between brain areas and is typically considered to reflect the functional connectivity among subnetworks of brain cells that engage in common processes^{1–3}. The existence of these functional large-scale networks raises an important question about the precise mechanisms underlying their emergence in local circuit operations. Specifically, how does phase-synchronized activity relate to local circuit operations that support the selection of inputs on the one hand, and the integration of diverse information streams on the other hand^{4–6}?

We survey here recent insights into these questions by reviewing the structural basis of rhythmic activity in precise cellular and circuit motifs and showing how their dynamic activation can implement canonical computations during states of rhythmic activation. We then propose a tripartite approach that combines three elements into a single dynamic motif to understand how circuit activation supports neuronal computations (Fig. 1a). First, the motif identifies the physical structure that is defined by its cellular and synaptic properties of its constituent cells (Fig. 1b) and by their local connectivity schemes (Fig. 1c). Second, a dynamic motif specifies the electrophysiological signature

by which it operates—for example, the modulation of neuronal firing, spike output synchronization or combinations thereof. This neurophysiological signature follows from the timescales and dynamics of cell-intrinsic conductances or synaptic mechanisms that impose frequency content on the motifs presented in this review. The third aspect of dynamic motifs describes the computational function, which is determined by the transformation of synaptic inputs the circuit performs. Simple circuits perform generic gain and scaling operations on their inputs⁷ (Fig. 2a). Circuits implement these generic computations as a function of the circuit elements (specific cell types) and as a function of the activation state of the brain at the time when input arrives (Fig. 2b–d). Whether these computational operations serve regulatory (for example, homeostatic) functions or identifiable information-processing functions (integrating or gating inputs, or propagating or blocking them) is a major question that dynamic motifs help to answer (see below). We therefore explicitly conceptualize the interdependence of circuits, activation signatures and computations as tripartite dynamic motifs (Fig. 1a). Completion of a dynamic motif implies a unique link of a neuronal activation signature to a precise function by specifying the underlying mechanisms and how they link to frequency-specific activation. The strength and appeal of thinking in terms of dynamic motifs is the required, explicit detail of such linkages that can then be interrogated by direct manipulation (for example, optogenetics or pharmacology) to establish causality or delineate correlational dependencies of the structural motif, its state-specific activation signature and the functional consequences of the underlying computation.

At the core of a dynamic motif is the appreciation that common structural themes, such as feedforward and feedback inhibition, operate at specific timescales^{8,9}. For many specific circuit motifs, these timescales are not random but can emerge as rhythmic activation patterns that span narrow frequency ranges (Fig. 1c). Accordingly,

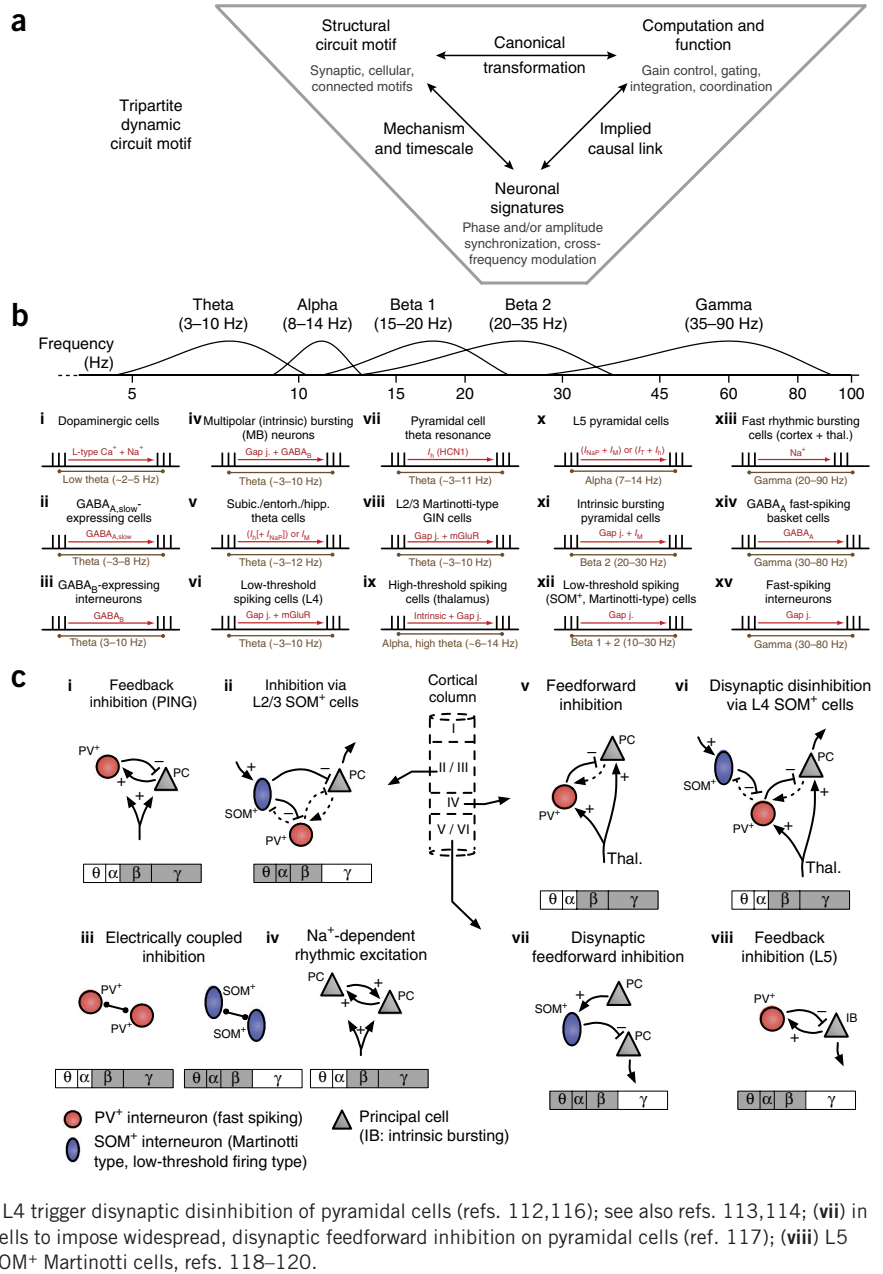
¹Department of Biology, York University, Toronto, Ontario, Canada. ²Centre for Vision Research, York University, Toronto, Ontario, Canada. ³Division of Fundamental Neurobiology, Toronto Western Research Institute, Toronto, Ontario, Canada. ⁴Division of Neurosurgery, Department of Surgery, University of Toronto, Toronto, Ontario, Canada. ⁵Brain Power, LLC, Boston, Massachusetts, USA. ⁶Department of Psychology, Harvard University, Cambridge, Massachusetts, USA. ⁷Department of Physics, University of Washington, Seattle, Washington, USA. ⁸Department of Neurosurgery, Stanford University, Stanford, California, USA. ⁹Donders Institute for Brain, Behavior, and Cognition, Radboud University Nijmegen, Nijmegen, the Netherlands. Correspondence should be addressed to T.W. (thiwom@yorku.ca).

Received 20 March; accepted 16 June; published online 28 July 2014;
doi:10.1038/nn.3764

Figure 1 Dynamic circuit motifs and the structural basis of several motifs with identified timescales. **(a)** Dynamic motifs represent a tight linkage of three components: the (1) circuit motif describes the structural basis (synaptic, cellular, local connectivity) that gives rise to (2) a characteristic neuronal activation signature, and (3) completion of a dynamic motif requires a link to a canonical input-output transformation that serves to implement a behavioral function.

(b) Synaptic and conductance-based properties of various cell types that have been identified experimentally to causally relate to the generation of and/or preferential engagement at timescales (frequencies) of rhythmic activity. The frequency range supported by each motif is indicated on the frequency axis. References: **i**, ref. 87; **ii**, refs. 88,89; see also refs. 90,91; **iii**, ref. 92; **iv**, ref. 93; **v**, refs. 94–96; **vi**, ref. 97; **vii**, ref. 98; **viii**, ref. 99; **ix**, refs. 32,100; **x**: codependence of alpha output on T current (I_T) and h current (I_h), ref. 101; codependence on persistent NaP current (I_{NaP}) and M current (I_M), refs. 102,103; **xi**, ref. 104; **xii**, ref. 82; **xiii**, refs. 105–108; for Na⁺ based high-threshold gamma bursting in thalamus see ref. 109; **xiv**, refs. 27,53,110; **xv**, ref. 111. Gap j., gap junction; mGluR, metabotropic glutamate receptor; subic./entorh./hipp., subicular, entorhinal and hippocampal.

(c) Overview of connected motifs that have been implicated as giving rise to oscillatory synchronized output of pyramidal cells. The frequency range most likely supported by each motif is indicated as gray shading in the frequency axis block below each motif. The laminar origins of the motifs are indicated in the center panel. Selected references: **(i)** gamma rhythmic feedback inhibition based on fast spiking interneurons, ref. 53; **(ii)** rhythmic inhibition through SOM⁺ L2/3 Martinotti-like cells spanning 3–10 Hz and 10–30 Hz, refs. 99,112; see also refs. 113,114; **(iii)** electrical gap junction-coupled synchrony in groups of fast-spiking cells (left) and LTS cells (right), refs. 82,97,111; **(iv)** see **b**, **xiii**; **(v)** the dominant gamma motif in cortical L4 is based on feedforward inhibition via fast spiking PV⁺ cells (refs. 16,115); **(vi)** SOM⁺ Martinotti-type cells in L4 trigger disinaptic disinhibition of pyramidal cells (refs. 112,116); see also refs. 113,114; **(vii)** in L5, SOM⁺ Martinotti cells are recruited by pyramidal cells to impose widespread, disinaptic feedforward inhibition on pyramidal cells (ref. 117); **(viii)** L5 feedback inhibition through low-threshold spiking or SOM⁺ Martinotti cells, refs. 118–120.



both brief rhythmic activity fluctuations and genuine longer-lasting and phase-coherent oscillatory activity can critically inform about the underlying circuit and its computational operation. We use this insight and show in the following how structural motifs translate into dynamic motifs that relate in explicit ways to underlying computational functions.

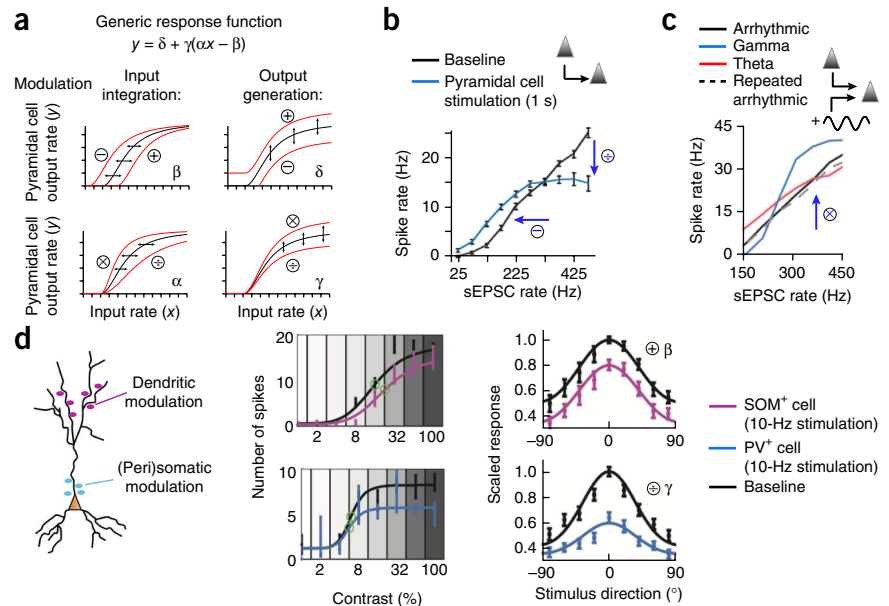
Feedforward inhibition and frequency-specific gain control

Feedforward inhibition (FFI) is one of the most fundamental organizational elements¹⁰ in the brain. It implements at its core a temporally structured normalization process of input to a circuit^{6,11} (Fig. 3a). Empirical and modeling work suggests that a generic FFI motif exists whose normalizing function selects synchronous inputs and facilitates their propagation^{12–14}. The FFI motif is implicated in circuits of information transfer between hippocampal subfields¹⁵, between thalamus and cortical layer (L) 4 (ref. 16), from cortical L4 and L5 to L2/3 (refs. 11,17), for cortico-striatal projections¹⁸ and for

cortico-cortical inter-areal interactions¹⁹ (see also ref. 6). The key components of the dynamic FFI motif are (1) strong excitatory connections to inhibitory neurons with (less) excitation to principal cells from the same source and (2) an inhibitory forward connection to principal cells with some time constant that imposes temporal structure on the FFI motif (Fig. 3a). This scheme efficiently extracts population-coded information among concomitant asynchronous inputs in situations when this input is oscillatory²⁰.

The generic FFI filtering network can be tuned to resonate at different frequencies by altering the inhibitory synaptic kinetics of the motif. The main physiological determinants of such frequency tuning of the FFI circuit are the passive and active membrane properties of the constituent cells²¹. For a subset of cell types, these intrinsic cellular properties actively pace their spike output rhythmically, irrespective of whether they receive asynchronous or temporally structured input. **Figure 1b** surveys intrinsic cellular features that have been implicated in tuning cells to generate rhythmic spike output with narrow band

Figure 2 Canonical computations of cortical circuits and generic response modulations supported by specific cell types. **(a)** The generic IO response function of a cortical cell entails four main parameters that determine either additive/subtractive changes of the IO relationship (β , δ), or scale the input (α) or output (γ) in a multiplicative/divisive way⁷. The panels show how pyramidal cell output rate (y axis) varies with increasing input rate (x axis) when the IO function parameters β , δ , α and γ are varied independently. **(b)** The spike rate of pyramidal cells in mouse frontal cortex as a function of the rate of simulated excitatory postsynaptic currents (sEPSC) during baseline condition (black) and when the pyramidal cell membrane is depolarized using light stimulation of a stable step-function opsin. **(c)** Output rate of a pyramidal cell in a dynamic clamp experiment in which current was injected to mimic the effect of EPSCs of increasing rate (x axis), and either without (black) or with oscillatory modulation of the input at 8 Hz (theta, red) or 40 Hz (gamma, blue). Blue arrows in **b,c** show sign and type of modulation. Modulation at gamma frequency increases the rate more effectively than theta frequency. **(d)** The effect of optogenetic stimulation of SOM⁺ (dendritic targeting) and PV⁺ (perisomatic targeting) interneurons in mouse visual cortex on the response of pyramidal cells (left) to stimuli of increasing contrast (middle) or varying stimulus motion direction (right). The former had an additive effect, whereas the latter had a multiplicative effect. Panel **b** adapted from ref. 64; **c** adapted from ref. 27; graphs in **d** adapted from ref. 65.



frequency content across all main frequency bands. This rhythmic tuning includes active pacemaking, often acting in concert with passive resonance^{22–24}, gap junctions and ephaptic mechanisms²⁵, as well as with synaptic connectivity to establish circuits that generate and sustain synchronized activity at specific frequencies^{5,26}. For a variety of small circuit motifs, the specific functional activation signatures they support have been described empirically, illustrating layer-specific expression and support for oscillatory activity at specific frequency bands (**Fig. 1c**).

In simulations using feedforward inhibition as a filter network, the primary determinants of the network's frequency selectivity is the resonant frequency of the feedforward interneuronal population and the time courses of the excitatory and inhibitory input received by excitatory cells²⁰. Physiological data support such a circuit property of tuned population resonance. Using expression of channelrhodopsin-2 in parvalbumin-positive (PV⁺) interneurons, gamma-frequency LFP oscillations were induced when PV⁺ cells were selectively activated with light pulses of random interpulse intervals²⁷. Thus, the input to these cells need not be oscillatory to induce gamma oscillations in the network. Such resonance also depended on excitatory synaptic transmission, suggesting that pyramidal cell activity was necessary for the manifestation of gamma oscillations. The time course of inhibition thereby not only specifies the filtering frequency, but is as well a critical determinant of the so-called synchrony threshold²⁸. This threshold determines to what degree synchrony at a particular frequency range must exist in the input to the dynamic motif for it to generate output. For the described gamma FFI motif, optogenetic manipulations have revealed that a sufficient level of gamma rhythmic input switches cells from a linear to a multiplicative input-output regime (**Fig. 2c**)²⁷. This finding suggests that an intrinsically gamma resonant circuit (in superficial cortical layers) implements a multiplicative gain control on gamma rhythmic input. Thus, not only does an FFI motif implement a synchrony filter, but it opens windows for supralinear, multiplicative gain modulation.

Simulations suggest that such gain control through a FFI motif for synchrony filtering is more robust to variations in input strength than

a high spike-threshold mechanism without inhibition, likely because of the additional computation of input normalization afforded by FFI²⁸. Synchrony filtering could thus support diverse biological functions that require the tuning of distant network nodes to a common temporal processing mode. Modeling work documents that such a tuning of nodes imposes a selection of oscillatory inputs to the exclusion of potentially distracting asynchronous population activity²⁰. In the following, we suggest that such an FFI-based input selection is likely realized by thalamo-cortical feedforward propagation of alpha-band activity.

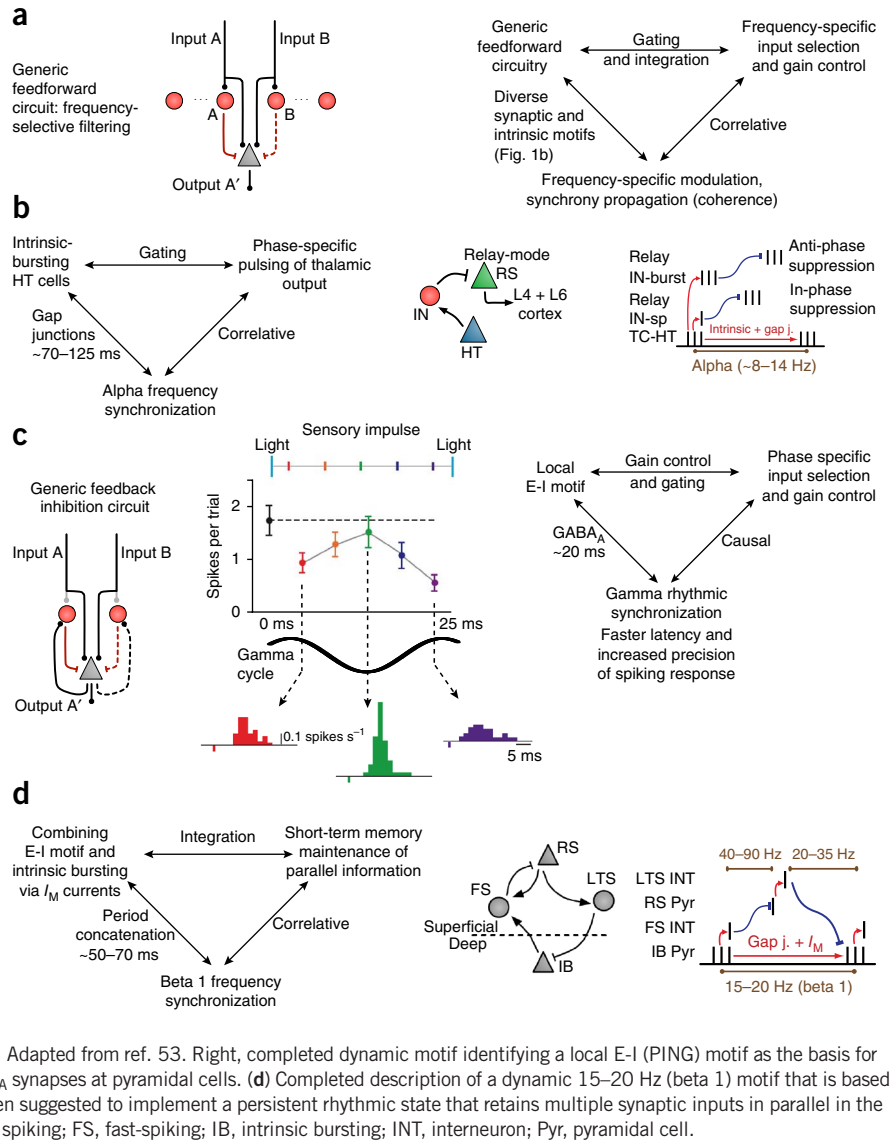
Distinct alpha rhythmic motifs amplify and suppress inputs

It is well documented that alpha rhythmic activity is a prominent signature of deep cortical layers in the primate neocortex^{29,30}. This cortical alpha band activity is tightly phase-locked to thalamic spiking activity, with enhanced spike–local field potential coherence for thalamo-cortical circuits processing attended visual input compared to reduced thalamo-cortical synchrony for neuronal circuits processing unattended input³¹. In awake primate recordings this attention-enhanced synchronization of cortical deep layer neurons to alpha rhythmic thalamic spike output is likely originating from alpha-paced thalamic excitation to the cortex³¹. In accord with these findings, the thalamo-cortical projections that carry an (asymmetric) alpha rhythmic excitation to cortical layers 4, 5 and 6 constitute a dynamic motif that is particularly well documented (**Fig. 3b** and **Supplementary Fig. 1**).

In particular, the main thalamo-cortical projections arise from relay-mode, regular spiking cells that are inhibited by a motif that is intrinsically rhythmic owing to gap junction–coupled high-threshold (HT) bursting neurons (**Fig. 3b**)³². These thalamic HT cells either elicit single spikes in interneurons, causing alpha rhythmic inhibition in phase with the alpha oscillation, or can elicit bursts of spikes in interneurons, resulting in anti-phase inhibition of the thalamic output projections (**Fig. 3b**, right). Accordingly, the relay-mode projection cells, which are otherwise arrhythmic, pulse their excitatory output

Figure 3 Dynamic circuit motifs activated at alpha, low beta and gamma frequencies that implement gain controls, gating and integration of inputs. **(a)** A generic FFI circuit (left) implementing frequency-specific gain modulation and selective routing of information based on an interplay of inhibitory synaptic timescales and the resonance properties of cells (right).

(b) Left, a completed dynamic motif that identifies gap junction coupling as the mechanism for synchronization. Center and right, the structural connectivity and temporal dynamics of the motif. The alpha rhythmic motif depends on rhythmically bursting, thalamo-cortical high-threshold (TC-HT) cells entraining inhibitory neurons (IN), which in turn impose rhythmic suppression onto relay-mode, regular spiking (RS) projection neurons. The bursting frequency of the HT cells depends on intrinsic currents, whereas the synchrony derives from coupling by gap junctions. Depending on whether the IN cells fire single spikes (IN-sp) or bursts (IN-burst), the relay cells are either in-phase suppressed or anti-phase suppressed. **(c)** Left, a generic feedback-inhibition circuit that realizes input selection. Dashed and gray lines denote ineffective connections. Center, experimental evidence that gamma synchronized activation in somatosensory cortex modulates the gain, precision and latency of responses to whisker stimulation (sensory impulse). A whisker was stimulated (colored vertical lines in top panel) at different phases relative to an optogenetically (blue light)-induced gamma oscillation. The spiking responses of pyramidal cells (y axis) varied as a function of the phase (x axis), with the largest, most precise and earliest responses obtained to impulses arriving at the trough of the gamma cycle (green dot and histogram), which is when the inhibition generated by the gamma oscillation is lowest. Histograms (bottom) show the spike count following the stimulation pulse (vertical colored ticks). Adapted from ref. 53. Right, completed dynamic motif identifying a local E-I (PING) motif as the basis for this gamma rhythmic gate. This motif depends on GABA_A synapses at pyramidal cells. **(d)** Completed description of a dynamic 15–20 Hz (beta 1) motif that is based on the coupling of two simpler motifs, and which has been suggested to implement a persistent rhythmic state that retains multiple synaptic inputs in parallel in the activated circuit. LTS, low-threshold spiking; RS, regular spiking; FS, fast-spiking; IB, intrinsic bursting; INT, interneuron; Pyr, pyramidal cell.



to cortical layers 4, 5, and 6 (ref. 33). Moreover, this thalamic alpha-generating motif has been causally linked to electroencephalographic alpha oscillations measured on the scalp³⁴.

The described excitatory thalamo-cortical alpha rhythmic motif and the observation of enhanced thalamo-cortical alpha-band synchronization during attention might at first sight appear to contradict empirical findings that show reduced local alpha activity in deep cortical layers processing attended information and enhanced local alpha band activity over cortices that are idling or processing unattended information^{29,30}. However, these putative discrepant findings can be resolved by postulating that two distinct dynamic motifs are activated for attended and unattended neuronal information. The first motif derives from observations that cortex processing unattended input shows an enhancement of alpha band power. We hypothesize that such intracortical alpha power increases in the absence of attention arise from a prominent alpha rhythmic source in L6 that is activated at the expense of an L4 cortico-thalamic activation during attention. L6 neurons resonate and intrinsically burst at alpha frequencies^{35,36}. Elegant optogenetic manipulations of L6 cells have shown that L6 neurons impose widespread columnar suppression through polysynaptic

inhibitory postsynaptic potentials by firing at the peak of local L6 excitation³⁷, which would correspond to the trough of alpha oscillations in L6. The L6 initiated putative alpha rhythmic inhibition likely spreads vertically into superficial layers as suggested by *in vivo* and *in vitro* studies^{29,38,39}. As a consequence, enhanced local alpha-rhythmic states of cortex reflect suppression of the cortical column's activity and reduced sensitivity and/or gain to input to the circuits. This dynamic motif of unattended cortex is akin to the concept of pulsed inhibition that predicts reduced responsiveness of cortical cells to synaptic inputs as a function of the phase of alpha oscillations⁴⁰. However, in contrast to an active pulsing of inhibition that originates outside of the cortical column, we propose that alpha-rhythmic inhibition follows from the lack of excitatory (thalamic) input. In particular, we suggest that pulsed inhibition reflects the unmasking of intrinsic alpha rhythmic inhibition originating from L6 cells^{29,36,37,39,41}. Furthermore, unlike a thalamically driven rhythm, this local cortical inhibitory motif could explain why cortical alpha oscillations can be easily entrained by transcranial alternating current stimulation⁴².

In contrast to the L6 inhibition motif, we suggest that a distinct, second thalamo-cortical motif becomes active during the processing of the

attended stimulus, displaying increased pulvinar spiking and concomitant enhancement of alpha pulvino-cortical coherence⁴³. Since pulvinar and thalamic output in general is largely concentrated to superficial layers⁴⁴, deep-layer inhibitory columnar drive (as described above) is overridden by thalamic drive to superficial layers through FFI to PV⁺ cells that generate gamma activity⁴⁵. Consistent with these results, superficial-layer gamma band synchronization is enhanced with attention in the primate brain⁴⁶ and can mediate long-range cortico-cortical interactions⁴⁷. The continuous cyclical inhibition from deep layers (see above) is evidenced as alpha-to-superficial-gamma cross-frequency coupling that occurs during both unattended⁴⁸ and attended states (see Supplementary Fig. 3 in ref. 31), which likely underlies alpha-phase modulated perceptual and working memory performances (reviewed in ref. 49).

In summary, the dynamic motif perspective suggests that selective attention is implemented in visual cortex by switching on two independent dynamic motifs: first, a thalamic alpha motif (Fig. 3b) that amplifies transmission of attended sensory information, and second, a release of an inhibitory, intracortical motif in L6 of cortical columns processing irrelevant information and reflecting the lack of thalamic drive.

Feedback inhibition and phase-selective gating of inputs

The previous section illustrated how a generic FFI motif implements frequency-specific filtering and gain control at gamma-band frequencies and how cell-specific, intrinsic alpha motifs link to (thalamically based) attentional amplification and (L6 based) inhibition of neuronal information transfer. These dynamic motifs are complemented by a generic feedback inhibition motif activated upon high beta and gamma frequency activity in superficial cortical layers (Fig. 1c, i). This dynamic pyramidal-interneuron gamma (PING) motif has been well characterized, both neurophysiologically and computationally^{50–52}. The PING motif depends on depolarizing input to pyramidal cells that excite PV⁺ interneurons, which project feedback inhibition on the pyramidal cells (Fig. 3c). The oscillation frequency of the PING motif depends on the GABA_A-ergic inhibition timescale and the overall level of excitation that determines when (and how fast) pyramidal cells recover from inhibition to reactivate the interneurons (Fig. 3c).

This superficial-cortex PING motif is causally implicated⁵³ as gating sensory inputs as a function of the phase in gamma cycle^{54,55}. In an elegant experiment, Cardin *et al.* used light to control gamma oscillations by light-stimulating PV⁺ interneurons and recorded from pyramidal cell populations while rodents' whiskers were stimulated at different phases of the gamma cycle⁵³. Interconnected pyramidal cells responded to sensory input at phases in the gamma cycle that corresponded to the lowest level of inhibition with the maximal spike rate, fastest latency and highest precision (lowest variability) (Fig. 3c, center). These response modulations highlight the computational role of the gamma cycle in implementing phase-dependent gain modulation of synaptic inputs by imposing brief time windows of maximal sensitivity to input and maximal efficacy of output (evident in the number and precision of generated spikes). Thus, computationally, the same synaptic inputs will result in enhanced spike output in the presence of gamma rhythmic modulation, a phenomenon that has been explained by the reduced temporal variability of inhibition generated in the interneuron population⁵⁶. Such a temporal tightening of inhibition effectively allows higher depolarization levels and a steeper rise of the pyramidal neurons' membrane potential in response to incoming excitatory synaptic potentials^{56,57}. As a consequence, pyramidal cells generate spike output not only more precisely but also with a higher spike probability during gamma rhythmic inhibition⁵⁸.

The delineated gating mechanism of the gamma PING motif is very likely a canonical motif used widely in the primate brain for the selective routing of information^{46,59}. At the mesoscale of activated cortical columns, gamma synchrony has been shown to index selective neuronal communication^{59,60}. Gamma synchronization predicts which inputs are selected and which local groups of neurons communicate (Supplementary Fig. 2). At the single-cell level, a recent study has provided mechanistic support for gamma-mediated gating during attentional processing⁴⁶. This study revealed that putative interneurons in area V4 of the macaque are gamma phase-locked most strongly (about twice as strongly as pyramidal cells) and spike readily at gamma frequencies even before the processing of bottom-up induced visual stimulation (Supplementary Fig. 3). Notably, when bottom-up visual input was present (after stimulus onset), the putative interneurons showed all main characteristics needed to implement a selective gate on the feedforward inputs. First, they began to phase lock at slightly later phases than principal cells. This suggests that interneurons receive excitation from principal cells and feed back inhibition onto them (consistent with a PING motif). Second, gamma locking was stronger when cells processed attentionally selected input rather than irrelevant input, replicating enhanced selective gamma locking as a function of stimulus relevance⁶¹. And third, the gamma attention effect interacted with the activation of the cells, showing a strong gating effect only for cells and sites that were firing to (that is, were tuned to) the stimulus, but reduced gamma locking for cells with low firing rates (Supplementary Fig. 3d,e). This activation-dependent attention effect suggests a push-pull mechanism of stimulus selection. Such a push-pull effect is reminiscent of the decorrelation of activity of cell populations in *in vitro* studies⁶². In particular, this work suggests that pyramidal cells receive strongly synchronous input from only subsets of interneurons but that neighboring interneurons do not necessarily spike synchronously, allowing an interneuron-mediated decorrelation of principal cells firing for the attended versus the unattended stimulus information⁶³. In summary, the gamma-rhythmic, dynamic PING motif activated in superficial cortical layers implements the selection of inputs by enhancing the throughput of attended information and reducing the impact of the firing and synchrony of unselected cells.

Gain control and cell-type specificity of rhythmic motifs

The studies discussed have in common that a computational function is associated with the rhythmic activation of a structural motif. The significance of this association—that is, the role of oscillatory activity in realizing gain control in cortical circuits—is exemplified by comparing directly the differential effect of tonic versus oscillatory membrane potential depolarization. By artificially elevating the excitation-inhibition (E-I) balance of a circuit over a timescale of several seconds, a recent optogenetic study succeeded in showing that tonic depolarization of pyramidal cells enhances their sensitivity but causes early saturation of spiking responses to synaptic input (a subtractive and divisive effect on the input-output (IO) curve)⁶⁴ (Fig. 2b). In contrast to this dysfunctional effect of prolonged depolarization of pyramidal cells, short-lasting, arrhythmic activation of pyramidal cells in mouse frontal cortex using the dynamic clamp technique to represent asynchronous synaptic inputs does not change the IO relationship (Fig. 2c)²⁷. However, when synaptic inputs to a pyramidal cell are modulated with a 40-Hz gamma oscillation, a notable multiplicatively increased response gain becomes evident that is accompanied by reduced variability in the spiking output of the cell (Fig. 2c)²⁷. Such gain modulation is not seen with slower (theta) input modulation.

This evidence suggests that rhythmic activation of a motif can indeed endow a circuit with a function that the circuit does not necessarily reveal in the arrhythmic state. However, one should bear in mind that a motif's function can in principle be activated without sustained oscillatory entrainment¹¹. This has been elegantly documented in optogenetic studies of the gain control function of GABAergic PV⁺ basket cells that form the dynamic PING gamma motif and the superficial-layer SOM⁺ cells that are implicated in alpha and beta rhythmic entrainment of principal cells (see Fig. 1b,c)^{65,66}. For example, Wilson *et al.*⁶⁵ stimulated mouse visual cortex with visual gratings of increasing contrasts and varying motion directions at the same time as populations of dendritic targeting SOM⁺ interneurons or populations of fast-spiking PV⁺ interneurons were optically activated in a 10-Hz rhythm. Optical activation of the interneuron cell classes affected the IO function of principal cells differentially (Fig. 2d). Light-induced, synchronized inhibition of dendrite targeting interneurons broadened the direction selectivity of principal cells and suppressed contrast and direction tuning functions, representing a subtractive effect on the IO curve (Fig. 2a). In contrast, inhibition mediated by 10-Hz PV⁺ cell activation had a divisive influence on sensory inputs, scaling the response functions down without changing selectivity⁶⁵. Taken together, the scaling and shifting of the IO function of pyramidal cells can be traced back to inhibitory cell types in the neocortical microcircuit, PV⁺ and SOM⁺ cells⁶⁶, that are each implicated in synchronizing principal cell output at alpha, beta and gamma frequencies (see Fig. 1b,c).

Combining cell-specific and circuit-based dynamic motifs

Beyond cell type specificity of single dynamic motifs, a recent set of studies succeeded in showing how two simple motifs can be combined to implement a specific computational function that is possibly realized in cross-layer interactions. In particular, Kopell *et al.* used *in vitro* electrophysiology, pharmacology and modeling to identify a 15–20 Hz oscillatory motif that combines an intrinsic bursting cell motif in deep layers with a superficial PING feedback inhibition motif⁶⁷. During dynamic activation this motif computationally integrates diverse inputs and maintains these inputs in a short-term memory buffer in principal cell spiking activity—without a competitive, selective gating that would follow from PING motif activation alone (Fig. 3d). This beta 1 dynamic circuit motif is instantiated in the slice when the afferent, excitatory drive to an E-I gamma motif in the superficial layer is decreased pharmacologically to such an extent that feedback inhibition from basket cells does not induce gamma-band oscillations in superficial cortex^{68,69}. In this low excitation regime, the superficial E-I motif is activated by deep-layer cells that intrinsically burst at a high, 20–30 Hz beta inter-burst frequency (see Fig. 1b, xi). When superficial excitatory cells recover from inhibition, they excite a subclass of Martinotti cells, the low-threshold spiking (LTS) cells, whose dendritic inhibition of deep-layer burst neurons slows (resets) their burst frequency⁶⁹ (Fig. 3d, center and right). The result of this coupling of an E-I motif and an intrinsic burst motif by LTS cells is an ~15-Hz oscillation that can be sustained during low excitation. Modeling studies of this dynamic circuit have shown that it allows two separable inputs to remain segregated by distinct populations of pyramidal cells firing at distinct phases of the beta 1 oscillation⁶⁷. These dynamic circuit properties suggest that the beta 1 motif is recruited by brain circuits when information from parallel input streams is received, either in the absence of or after strong superficial-layer excitation that would impose a selection of inputs. It remains speculative, however, whether the beta 1 dynamic circuit underlies the observed 15-Hz oscillation signature that has recently

been reported to index working memory maintenance, decision confidence, choice behavior or long-range sensorimotor integration before perceptual decision making^{2,70,71}. The outlined motif, however, does provide a precise hypothesis for future tests, including the prediction that cell firing at distinct 15–20 Hz beta frequency phases conveys information about distinct input streams and independent of firing rate modulation in the circuit⁶⁷.

Rhythmic dynamic motifs indexing context-dependent gating

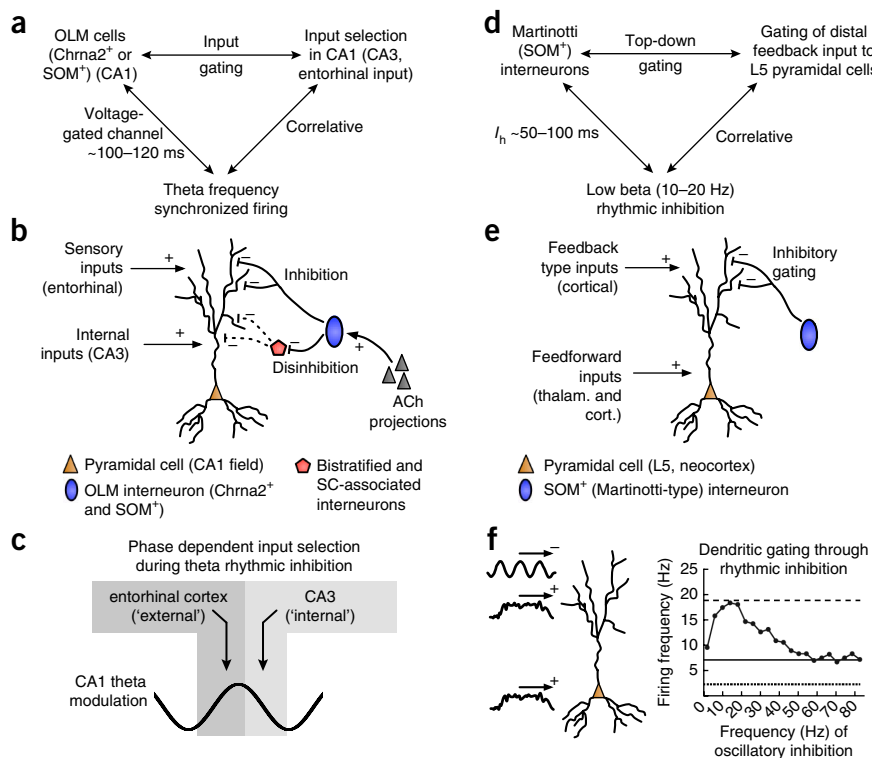
So far we discussed dynamic motifs that amplify or suppress inputs, gate one among many inputs or integrate diverse inputs—all indexed through rhythmic activation (Fig. 3a–d). These dynamic motifs are activated only during specific behavioral states—that is, their activation is context dependent. Recent studies suggest that such context-specific gating of information flow can be achieved with a common motif based on dendritic inhibition and disinhibition of pyramidal cells^{72–75}. We outline two example motifs of such dynamic 'dendritic' switches (Fig. 4). One motif, involving oriens lacunosum-moleculare (OLM) cells in the hippocampal CA1 field, is measurable in rhythmic entrainment of switch cells themselves (Fig. 4a–c), and the other example, a SOM⁺-cell switch in superficial neocortex, uses rhythmic inhibitory entrainment of pyramidal cell dendrites to implement a frequency-specific switch of information outflow from L5 cells (Fig. 4d–f).

In the hippocampal CA1 field, OLM interneurons have been suggested to establish a disinhibitory switch for pyramidal cell activation^{73,76}. Pyramidal cells in CA1 receive inputs from entorhinal cortex distally, whereas input from the Schaffer collaterals from CA3 targets more proximal dendrites (Fig. 4b). Mirroring this setup, OLM interneurons directly inhibit distal dendrites, but they indirectly, by way of bistratified and stratum radiatum interneurons, disinhibit the more proximal part. As a consequence, activating OLM cells in the CA1 field turns the gate toward decoding putative memory-related information from the CA3 field and away from processing sensory inputs arriving at distal dendrites from the entorhinal cortex⁷⁶. Identified sources of OLM activation are cholinergic inputs from the fimbria fornix and medial septum, suggesting that the neuromodulatory tone of acetylcholine via nicotinic receptors influences whether the OLM-mediated gate is effective.

OLM cells are known to strongly modulate their firing at theta frequencies and have been implicated as supporting theta-gamma coupling in the hippocampus^{77,78}. This rhythmic activation of OLM cells suggests that the gating depends on the phase at which they prefer to fire⁷⁹. When OLM cells fire at the peak of a theta oscillation, the gate is expected to favor CA3 inputs, whereas CA1 cells should become most sensitive to entorhinal inputs when the peak inhibition via OLM cells has decayed (Fig. 4c). In summary, an OLM-cell dependent and theta-rhythmic gate in the CA1 field of the hippocampus could provide a dynamic motif that parses information from different sources into distinct phases of the theta cycle. Such a parsing may functionally be used, for example, for segregating sensory encoding (via entorhinal cortex) from memory retrieval (via CA3)⁸⁰.

Beyond the hippocampus, dendritic gating of inputs to pyramidal cells reflects a canonical dynamic motif in the neocortex⁷². Cortical L5 pyramidal cells receive feedback-type inputs from higher order cortices and modulatory input from the thalamus through their distal dendritic arbors in superficial L1. Two key questions arise in such a design, where the majority of L1 inputs carry context-specific, 'top-down' information: first, how can dendritic input activate the L5 cell effectively, and second, how can L1 feedback input bias or route L5 cell activity in response to somatic (feedforward-type) inputs? Detailed biophysical modeling have shown that an answer to both

Figure 4 Gating of distal and proximal dendritic information streams through rhythmic inhibition at theta frequencies in the hippocampus and at 10–20 Hz in the neocortex. (a–c) Dynamic motif of theta rhythmic gating of pyramidal cell inputs in CA1 through OLM interneurons. (a) Dynamic motif of OLM cell-based gating of information flow. OLM cells are highly specific in expressing *Chrna2* but coexpress SOM with several other cell types. (b) Schematic of distal and proximal inputs to a CA1 pyramidal cell. These inputs are gated by direct (OLM cell) inhibition and indirect (OLM cell-mediated) disinhibition. A source for this gating is cholinergic (ACh) neuromodulation, likely via the fornix⁷⁶. SC, Schaffer collateral. (c) The dendritic gate may switch during the theta cycle, thereby parsing information depending on the phase at which input arrives relative to the OLM cell firing (see main text). (d–f) Dynamic motif of dendritic gating of neocortical L5 cell activation. Rhythmic inhibition at 10–20 Hz at distal dendritic arbors facilitates excitatory feedback-type inputs to influence the L5 cell and to facilitate spiking responses to somatic inputs. The dashed line indicates the neuron's mean firing rate with proximal (basal) and distal excitation, but without distal inhibition. The dotted line represents the neuron's mean firing rate with proximal (basal) excitation only. Right panel in f adapted from ref. 81, Li, X., Morita, K., Robinson, H.P. & Small, M. Control of layer 5 pyramidal cell spiking by oscillatory inhibition in the distal apical dendrites: a computational modeling study. *J. Neurophysiol.* **109**, 2739–2756 (2013) (see main text).



questions must take into account the passive 15–20 Hz resonance of distal dendrites of L5 pyramidal cells that can be traced to afterhyperpolarizing I_h conductances⁸¹ (Fig. 4d). As a result of these passive resonance properties at distal dendrites, rhythmic 15–20 Hz inhibition of L5 dendrites gates excitatory feedback input to the L5 cells: rhythmic inhibition determines whether spiking output is generated in response to simultaneously presented somatic (feedforward-type) inputs (Fig. 4d–f) and, furthermore, it can make the L5 cell fire even in the absence of bottom-up, somatic depolarization⁸¹. Empirical studies suggest that distal dendritic gating is realized by activating LTS-type or other Martinotti-type cells, which support synchronized firing at 5–30 Hz frequencies⁸² (see also ref. 81).

In summary, feedback gating through dendritic L5 gating constitutes a complete dynamic motif that provides an explicit scenario for how top-down inputs affect local processing (Fig. 4d). It will be important to empirically validate the role and identity of specific cell types in generating rhythmic dendritic inhibition at the time when feedback input and feedforward input are combined in a cortical column^{72,83}.

Conclusion

We have documented a dynamic circuit motif framework that links structure, physiological activation signature and computation in tripartite motifs. We focused on motifs that become measurable in rhythmically synchronized activity, documenting that synchronized activation is only poorly described with regard to a unified frequency axis or in terms of simplified general functional attributes. Rather, we have shown that at the same timescale and frequency, such as alpha-frequency activation, distinct circuit motifs realize distinct computational operations.

A fundamental future challenge will be to precisely identify how tight rhythmic circuit operations relate to computations and their consequences for behavior. For example, rhythmic activation may

not be necessary for a specific computation (as its ‘cause’), but rather may reliably accompany the consequences of the computation. At another extreme, rhythmic activation can be ‘anti-computational’, reflecting unfolding dynamics of a complex system, as is evident in seizure activity and also in so-called ‘ringing’ that can materialize as gamma bursts following transient thalamic current stimulation⁸⁴. The dynamic circuit motifs concept makes explicit that these questions about the relation of rhythmically active motifs to the computation are genuine experimental questions. By knowing the underlying oscillatory mechanism through the motifs, synchrony components may be reduced optogenetically or pharmacologically, while keeping the circuit functional (for example, ref. 85). When computations disappear in such a situation, the synchronous activation can be said to be causal; otherwise, it can be identified as a correlational or spurious linkage. Taken together, we believe that dynamic circuit motifs serve as the critical building blocks for developing a taxonomy of oscillations not in terms of a rigid frequency scale but according to the specific computational operations that are implemented through synchronized activation of neuronal circuits⁸⁶.

Note: Any Supplementary Information and Source Data files are available in the online version of the paper.

ACKNOWLEDGMENTS

We are grateful to the speakers of two workshops held at the Computational and Systems Neuroscience (cosyne.org) meetings on The Consequences of Brain Rhythms in the Organization of Neuronal Computation (2009) and Developing Simplified Algebras to Describe Large-Scale Brain Dynamics (2011) for numerous discussions. We thank T. Donner, C. Eliasmith, B. Hansen and M. Vinck for discussions and comments on an earlier version of the manuscript. T.W. was supported by grants from the Canadian Institutes of Health Research (CIHR), the Natural Sciences and Engineering Research Council of Canada (NSERC) and the Ontario Ministry of Economic Development and Innovation (MEDI). T.A.V. was supported by grants from the CIHR. N.T.S. was supported by US National

Institutes of Health (NIH) R01 grants NS18741, NS44623 and grant HD 18381, NIH Institutional Training Grant T32 MH070328, and the US National Center for Research Resources (P41 RR14075). P.T. was supported by a grant from the Netherlands Organization for Scientific Research (NWO) Computational Lifesciences program and by Neuroseeker (FP7 grant agreement 600925).

COMPETING FINANCIAL INTERESTS

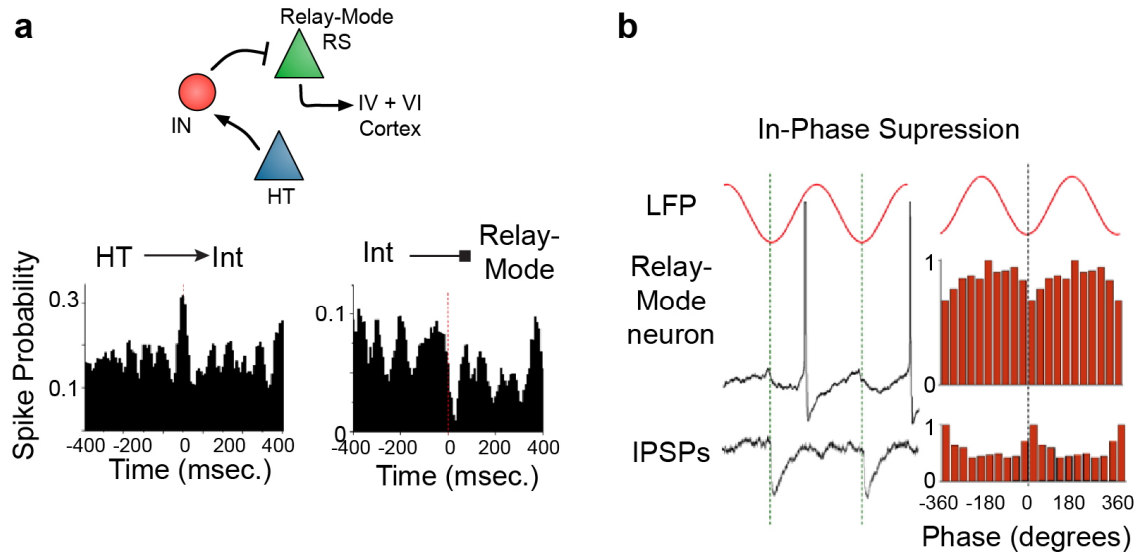
The authors declare no competing financial interests.

Reprints and permissions information is available online at <http://www.nature.com/reprints/index.html>.

1. Fell, J. & Axmacher, N. The role of phase synchronization in memory processes. *Nat. Rev. Neurosci.* **12**, 105–118 (2011).
2. Siegel, M., Donner, T.H. & Engel, A.K. Spectral fingerprints of large-scale neuronal interactions. *Nat. Rev. Neurosci.* **13**, 121–134 (2012).
3. Buzsáki, G. & Wang, X.J. Mechanisms of gamma oscillations. *Annu. Rev. Neurosci.* **35**, 203–225 (2012).
4. Tiesinga, P., Fellous, J.M. & Sejnowski, T.J. Regulation of spike timing in visual cortical circuits. *Nat. Rev. Neurosci.* **9**, 97–107 (2008).
5. Grillner, S., Markram, H., De Schutter, E., Silberberg, G. & LeBeau, F.E. Microcircuits in action—from CPGs to neocortex. *Trends Neurosci.* **28**, 525–533 (2005).
6. Akam, T. & Kullmann, D.M. Oscillatory multiplexing of population codes for selective communication in the mammalian brain. *Nat. Rev. Neurosci.* **15**, 111–122 (2014).
7. Silver, R.A. Neuronal arithmetic. *Nat. Rev. Neurosci.* **11**, 474–489 (2010).
8. Karnani, M.M., Agetsuma, M. & Yuste, R. A blanket of inhibition: functional inferences from dense inhibitory connectivity. *Curr. Opin. Neurobiol.* **26C**, 96–102 (2014).
9. Wang, X.J. Neurophysiological and computational principles of cortical rhythms in cognition. *Physiol. Rev.* **90**, 1195–1268 (2010).
10. Kepecs, A. & Fishell, G. Interneuron cell types are fit to function. *Nature* **505**, 318–326 (2014).
11. Bruno, R.M. Synchrony in sensation. *Curr. Opin. Neurobiol.* **21**, 701–708 (2011).
12. Pouille, F., Marin-Burgin, A., Adesnik, H., Atallah, B.V. & Scanziani, M. Input normalization by global feedforward inhibition expands cortical dynamic range. *Nat. Neurosci.* **12**, 1577–1585 (2009).
13. Kremkow, J., Aertsen, A. & Kumar, A. Gating of signal propagation in spiking neural networks by balanced and correlated excitation and inhibition. *J. Neurosci.* **30**, 15760–15768 (2010).
14. Kremkow, J., Perrinet, L.U., Masson, G.S. & Aertsen, A. Functional consequences of correlated excitatory and inhibitory conductances in cortical networks. *J. Comput. Neurosci.* **28**, 579–594 (2010).
15. Zemankovics, R., Veres, J.M., Oren, I. & Hajos, N. Feedforward inhibition underlies the propagation of cholinergically induced gamma oscillations from hippocampal CA3 to CA1. *J. Neurosci.* **33**, 12337–12351 (2013).
16. Cruikshank, S.J., Urabe, H., Nurmikko, A.V. & Connors, B.W. Pathway-specific feedforward circuits between thalamus and neocortex revealed by selective optical stimulation of axons. *Neuron* **65**, 230–245 (2010).
17. Thomson, A.M. & Bannister, A.P. Interlaminar connections in the neocortex. *Cereb. Cortex* **13**, 5–14 (2003).
18. Kumar, A., Vlachos, I., Aertsen, A. & Boucsein, C. Challenges of understanding brain function by selective modulation of neuronal subpopulations. *Trends Neurosci.* **36**, 579–586 (2013).
19. Lee, A.T. *et al.* Pyramidal neurons in prefrontal cortex receive subtype-specific forms of excitation and inhibition. *Neuron* **81**, 61–68 (2014).
20. Akam, T. & Kullmann, D.M. Oscillations and filtering networks support flexible routing of information. *Neuron* **67**, 308–320 (2010).
21. Timofeev, I., Bazhenov, M., Seigneur, J. & Sejnowski, T. Neuronal synchronization and thalamocortical rhythms in sleep, wake and epilepsy. in *Jasper's Basic Mechanisms of the Epilepsies* (eds. Noebels, J.L., Avoli, M., Rogawski, M.A., Olsen, R.W. & Delgado-Escueta, A.V.) (National Center for Biotechnology Information, Bethesda, Maryland, USA, 2012).
22. Hutcheon, B. & Yarom, Y. Resonance, oscillation and the intrinsic frequency preferences of neurons. *Trends Neurosci.* **23**, 216–222 (2000).
23. Otte, S., Hasenstaub, A. & Callaway, E.M. Cell type-specific control of neuronal responsiveness by gamma-band oscillatory inhibition. *J. Neurosci.* **30**, 2150–2159 (2010).
24. Lawrence, J.J. Cholinergic control of GABA release: emerging parallels between neocortex and hippocampus. *Trends Neurosci.* **31**, 317–327 (2008).
25. Fröhlich, F. & McCormick, D.A. Endogenous electric fields may guide neocortical network activity. *Neuron* **67**, 129–143 (2010).
26. Moca, V.V., Nikolic, D., Singer, W. & Muresan, R.C. Membrane resonance enables stable and robust gamma oscillations. *Cereb. Cortex* **24**, 119–142 (2014).
27. Sohal, V.S., Zhang, F., Yizhar, O. & Deisseroth, K. Parvalbumin neurons and gamma rhythms enhance cortical circuit performance. *Nature* **459**, 698–702 (2009).
28. Patel, M. & Joshi, B. Decoding synchronized oscillations within the brain: phase-delayed inhibition provides a robust mechanism for creating a sharp synchrony filter. *J. Theor. Biol.* **334**, 13–25 (2013).
29. Bollimunta, A., Mo, J., Schroeder, C.E. & Ding, M. Neuronal mechanisms and attentional modulation of corticothalamic alpha oscillations. *J. Neurosci.* **31**, 4935–4943 (2011).
30. Buffalo, E.A., Fries, P., Landman, R., Buschman, T.J. & Desimone, R. Laminar differences in gamma and alpha coherence in the ventral stream. *Proc. Natl. Acad. Sci. USA* **108**, 11262–11267 (2011).
31. Saalmann, Y.B., Pinsk, M.A., Wang, L., Li, X. & Kastner, S. The pulvinar regulates information transmission between cortical areas based on attention demands. *Science* **337**, 753–756 (2012).
32. Lorincz, M.L., Kekesi, K.A., Juhász, G., Crunelli, V. & Hughes, S.W. Temporal framing of thalamic relay-mode firing by phasic inhibition during the alpha rhythm. *Neuron* **63**, 683–696 (2009).
33. Constantinople, C.M. & Bruno, R.M. Deep cortical layers are activated directly by thalamus. *Science* **340**, 1591–1594 (2013).
34. Hughes, S.W. *et al.* Thalamic gap junctions control local neuronal synchrony and influence macroscopic oscillation amplitude during EEG alpha rhythms. *Front. Psychol.* **2**, 193 (2011).
35. Silva, L.R., Amitai, Y. & Connors, B.W. Intrinsic oscillations of neocortex generated by layer 5 pyramidal neurons. *Science* **251**, 432–435 (1991).
36. Castro-Alamancos, M.A. & Rigas, P. Synchronized oscillations caused by disinhibition in rodent neocortex are generated by recurrent synaptic activity mediated by AMPA receptors. *J. Physiol. (Lond.)* **542**, 567–581 (2002).
37. Olsen, S.R., Bortone, D.S., Adesnik, H. & Scanziani, M. Gain control by layer six in cortical circuits of vision. *Nature* **483**, 47–52 (2012).
38. Castro-Alamancos, M.A. & Oldford, E. Cortical sensory suppression during arousal is due to the activity-dependent depression of thalamocortical synapses. *J. Physiol. (Lond.)* **541**, 319–331 (2002).
39. Florez, C.M. *et al.* *In vitro* recordings of human neocortical oscillations. *Cereb. Cortex* doi:10.1093/cercor/bht235 17 September (2013).
40. Jensen, O. & Mazaheri, A. Shaping functional architecture by oscillatory alpha activity: gating by inhibition. *Front. Hum. Neurosci.* **4**, 186 (2010).
41. Fischer, I. *et al.* Zero-lag long-range synchronization via dynamical relaying. *Phys. Rev. Lett.* **97**, 123902 (2006).
42. Helfrich, R.F. *et al.* Entrainment of brain oscillations by transcranial alternating current stimulation. *Curr. Biol.* **24**, 333–339 (2014).
43. Saalmann, Y.B. & Kastner, S. Cognitive and perceptual functions of the visual thalamus. *Neuron* **71**, 209–223 (2011).
44. Sherman, S.M. & Guillery, R.W. *Exploring the Thalamus and its Role in Cortical Function* (MIT Press, 2006).
45. Petersen, C.C. & Crochet, S. Synaptic computation and sensory processing in neocortical layer 2/3. *Neuron* **78**, 28–48 (2013).
46. Vinck, M., Womelsdorf, T., Buffalo, E.A., Desimone, R. & Fries, P. Attentional modulation of cell-class-specific gamma-band synchronization in awake monkey area V4. *Neuron* **80**, 1077–1089 (2013).
47. Gregoriou, G.G., Gotts, S.J. & Desimone, R. Cell-type-specific synchronization of neural activity in FEF with V4 during attention. *Neuron* **73**, 581–594 (2012).
48. Spaak, E., Bonnefond, M., Maier, A., Leopold, D.A. & Jensen, O. Layer-specific entrainment of gamma-band neural activity by the alpha rhythm in monkey visual cortex. *Curr. Biol.* **22**, 2313–2318 (2012).
49. Thut, G., Miniussi, C. & Gross, J. The functional importance of rhythmic activity in the brain. *Curr. Biol.* **22**, R658–R663 (2012).
50. de Almeida, L., Idiart, M. & Lisman, J.E. The input-output transformation of the hippocampal granule cells: from grid cells to place fields. *J. Neurosci.* **29**, 7504–7512 (2009).
51. Tiesinga, P. & Sejnowski, T.J. Cortical enlightenment: are attentional gamma oscillations driven by ING or PING? *Neuron* **63**, 727–732 (2009).
52. Börgers, C., Epstein, S. & Kopell, N.J. Gamma oscillations mediate stimulus competition and attentional selection in a cortical network model. *Proc. Natl. Acad. Sci. USA* **105**, 18023–18028 (2008).
53. Cardin, J.A. *et al.* Driving fast-spiking cells induces gamma rhythm and controls sensory responses. *Nature* **459**, 663–667 (2009).
54. Womelsdorf, T. *et al.* Orientation selectivity and noise correlation in awake monkey area V1 are modulated by the gamma cycle. *Proc. Natl. Acad. Sci. USA* **109**, 4302–4307 (2012).
55. Vinck, M. *et al.* Gamma-phase shifting in awake monkey visual cortex. *J. Neurosci.* **30**, 1250–1257 (2010).
56. Tiesinga, P.H. & Sejnowski, T.J. Mechanisms for phase shifting in cortical networks and their role in communication through coherence. *Front. Hum. Neurosci.* **4**, 196 (2010).
57. Knoblich, U., Siegle, J.H., Pritchett, D.L. & Moore, C.I. What do we gain from gamma? Local dynamic gain modulation drives enhanced efficacy and efficiency of signal transmission. *Front. Hum. Neurosci.* **4**, 185 (2010).
58. Azouz, R. & Gray, C.M. Adaptive coincidence detection and dynamic gain control in visual cortical neurons *in vivo*. *Neuron* **37**, 513–523 (2003).
59. Bosman, C.A. *et al.* Attentional stimulus selection through selective synchronization between monkey visual areas. *Neuron* **75**, 875–888 (2012).
60. Womelsdorf, T. *et al.* Modulation of neuronal interactions through neuronal synchronization. *Science* **316**, 1609–1612 (2007).
61. Womelsdorf, T., Fries, P., Mitra, P.P. & Desimone, R. Gamma-band synchronization in visual cortex predicts speed of change detection. *Nature* **439**, 733–736 (2006).



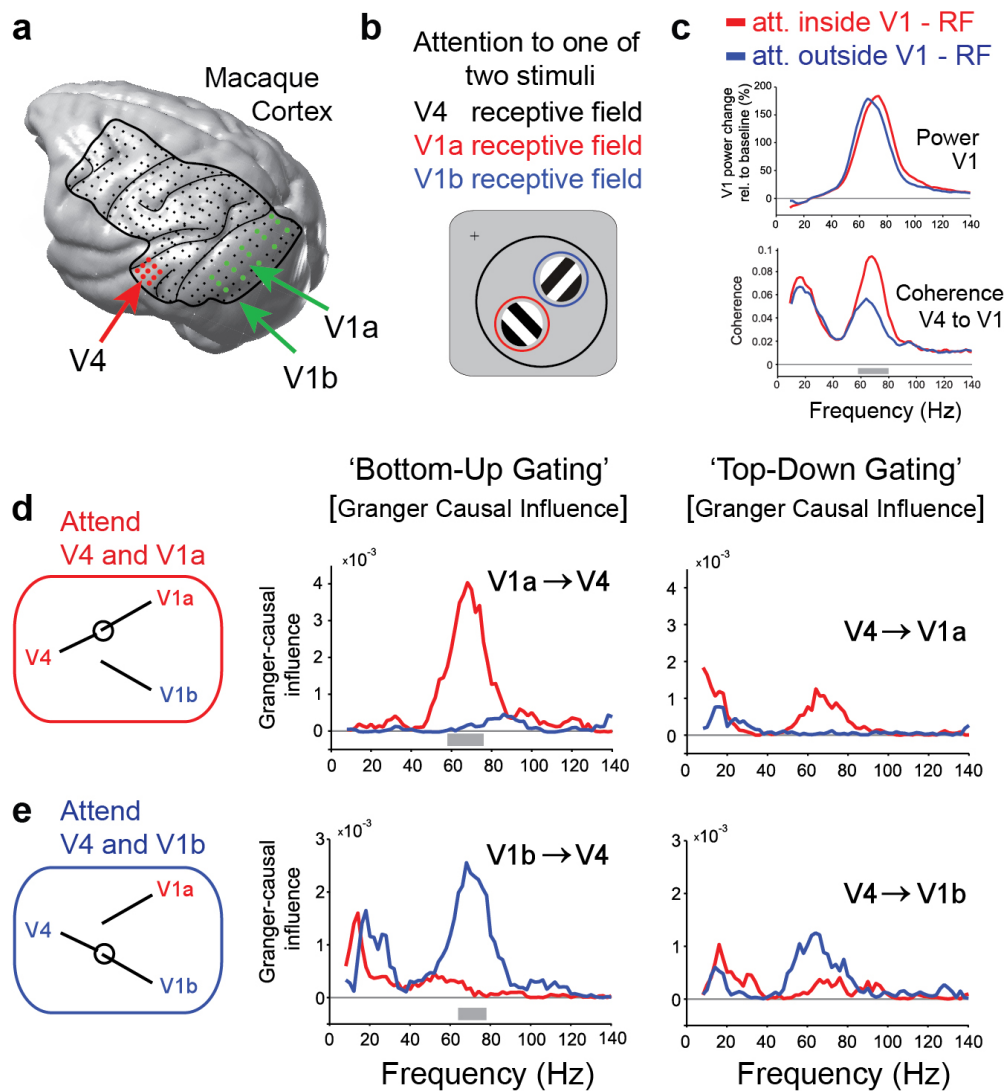
62. Sippy, T. & Yuste, R. Decorrelating action of inhibition in neocortical networks. *J. Neurosci.* **33**, 9813–9830 (2013).
63. Tetzlaff, T., Helias, M., Einevoll, G.T. & Diesmann, M. Decorrelation of neural-network activity by inhibitory feedback. *PLoS Comput. Biol.* **8**, e1002596 (2012).
64. Yizhar, O. *et al.* Neocortical excitation/inhibition balance in information processing and social dysfunction. *Nature* **477**, 171–178 (2011).
65. Wilson, N.R., Runyan, C.A., Wang, F.L. & Sur, M. Division and subtraction by distinct cortical inhibitory networks *in vivo*. *Nature* **488**, 343–348 (2012).
66. Lee, S.H., Kwan, A.C. & Dan, Y. Interneuron subtypes and orientation tuning. *Nature* **508**, E1–E2 (2014).
67. Kopell, N., Whittington, M.A. & Kramer, M.A. Neuronal assembly dynamics in the beta1 frequency range permits short-term memory. *Proc. Natl. Acad. Sci. USA* **108**, 3779–3784 (2011).
68. Kramer, M.A. *et al.* Rhythm generation through period concatenation in rat somatosensory cortex. *PLoS Comput. Biol.* **4**, e1000169 (2008).
69. Roopun, A.K. *et al.* Period concatenation underlies interactions between gamma and beta rhythms in neocortex. *Front. Cell. Neurosci.* **2**, 1 (2008).
70. Salazar, R.F., Dotson, N.M., Bressler, S.L. & Gray, C.M. Content-specific frontoparietal synchronization during visual working memory. *Science* **338**, 1097–1100 (2012).
71. Lipsman, N. *et al.* Beta coherence within human ventromedial prefrontal cortex precedes affective value choices. *Neuroimage* **85**, 769–778 (2014).
72. Larkum, M. A cellular mechanism for cortical associations: an organizing principle for the cerebral cortex. *Trends Neurosci.* **36**, 141–151 (2013).
73. Lovett-Barron, M. *et al.* Regulation of neuronal input transformations by tunable dendritic inhibition. *Nat. Neurosci.* **15**, 423–430 (2012).
74. Palmer, L., Murayama, P. & Larkum, M. Inhibitory regulation of dendritic activity *in vivo*. *Front. Neural Circuits* **6**, 26 (2012).
75. Wang, X.J., Tegner, J., Constantinidis, C. & Goldman-Rakic, P.S. Division of labor among distinct subtypes of inhibitory neurons in a cortical microcircuit of working memory. *Proc. Natl. Acad. Sci. USA* **101**, 1368–1373 (2004).
76. Leão, R.N. *et al.* OLM interneurons differentially modulate CA3 and entorhinal inputs to hippocampal CA1 neurons. *Nat. Neurosci.* **15**, 1524–1530 (2012).
77. Gloveli, T. *et al.* Differential involvement of oriens/pyramidal interneurons in hippocampal network oscillations *in vitro*. *J. Physiol. (Lond.)* **562**, 131–147 (2005).
78. Varga, C., Golshani, P. & Soltesz, I. Frequency-invariant temporal ordering of interneuronal discharges during hippocampal oscillations in awake mice. *Proc. Natl. Acad. Sci. USA* **109**, E2726–E2734 (2012).
79. Colgin, L.L. *et al.* Frequency of gamma oscillations routes flow of information in the hippocampus. *Nature* **462**, 353–357 (2009).
80. Hasselmo, M.E., Bodelon, C. & Wyble, B.P. A proposed function for hippocampal theta rhythm: separate phases of encoding and retrieval enhance reversal of prior learning. *Neural Comput.* **14**, 793–817 (2002).
81. Li, X., Morita, K., Robinson, H.P. & Small, M. Control of layer 5 pyramidal cell spiking by oscillatory inhibition in the distal apical dendrites: a computational modeling study. *J. Neurophysiol.* **109**, 2739–2756 (2013).
82. Mancilla, J.G., Lewis, T.J., Pinto, D.J., Rinzel, J. & Connors, B.W. Synchronization of electrically coupled pairs of inhibitory interneurons in neocortex. *J. Neurosci.* **27**, 2058–2073 (2007).
83. Jiang, X., Wang, G., Lee, A.J., Stornetta, R.L. & Zhu, J.J. The organization of two new cortical interneuronal circuits. *Nat. Neurosci.* **16**, 210–218 (2013).
84. Metherate, R. & Cruikshank, S.J. Thalamocortical inputs trigger a propagating envelope of gamma-band activity in auditory cortex *in vitro*. *Exp. Brain Res.* **126**, 160–174 (1999).
85. Robbe, D. & Buzsáki, G. Alteration of theta timescale dynamics of hippocampal place cells by a cannabinoid is associated with memory impairment. *J. Neurosci.* **29**, 12597–12605 (2009).
86. Buzsáki, G., Logothetis, N. & Singer, W. Scaling brain size, keeping timing: evolutionary preservation of brain rhythms. *Neuron* **80**, 751–764 (2013).
87. Drion, G., Massotte, L., Sepulchre, R. & Seutin, V. How modeling can reconcile apparently discrepant experimental results: the case of pacemaking in dopaminergic neurons. *PLoS Comput. Biol.* **7**, e1002050 (2011).
88. Hentschke, H. *et al.* Altered GABA_{A,slow} inhibition and network oscillations in mice lacking the GABA_A receptor β_3 subunit. *J. Neurophysiol.* **102**, 3643–3655 (2009).
89. White, J.A., Banks, M.I., Pearce, R.A. & Kopell, N.J. Networks of interneurons with fast and slow gamma-aminobutyric acid type A (GABA_A) kinetics provide substrate for mixed gamma-theta rhythm. *Proc. Natl. Acad. Sci. USA* **97**, 8128–8133 (2000).
90. Capogna, M. & Pearce, R.A. GABA_{A,slow} causes and consequences. *Trends Neurosci.* **34**, 101–112 (2011).
91. English, D.F. *et al.* GABAergic circuits mediate the reinforcement-related signals of striatal cholinergic interneurons. *Nat. Neurosci.* **15**, 123–130 (2012).
92. Molyneaux, B.J. & Hasselmo, M.E. GABA_B presynaptic inhibition has an *in vivo* time constant sufficiently rapid to allow modulation at theta frequency. *J. Neurophysiol.* **87**, 1196–1205 (2002).
93. Blatow, M. *et al.* A novel network of multipolar bursting interneurons generates theta frequency oscillations in neocortex. *Neuron* **38**, 805–817 (2003).
94. Chapman, C.A. & Lacaille, J.C. Intrinsic theta-frequency membrane potential oscillations in hippocampal CA1 interneurons of stratum lacunosum-moleculare. *J. Neurophysiol.* **81**, 1296–1307 (1999).
95. Glasgow, S.D. & Chapman, C.A. Conductances mediating intrinsic theta-frequency membrane potential oscillations in layer II parasubicular neurons. *J. Neurophysiol.* **100**, 2746–2756 (2008).
96. Boehlen, A., Henneberger, C., Heinemann, U. & Erchova, I. Contribution of near-threshold currents to intrinsic oscillatory activity in rat medial entorhinal cortex layer II stellate cells. *J. Neurophysiol.* **109**, 445–463 (2013).
97. Beierlein, M., Gibson, J.R. & Connors, B.W. A network of electrically coupled interneurons drives synchronized inhibition in neocortex. *Nat. Neurosci.* **3**, 904–910 (2000).
98. Stark, E. *et al.* Inhibition-induced theta resonance in cortical circuits. *Neuron* **80**, 1263–1276 (2013).
99. Fanselow, E.E., Richardson, K.A. & Connors, B.W. Selective, state-dependent activation of somatostatin-expressing inhibitory interneurons in mouse neocortex. *J. Neurophysiol.* **100**, 2640–2652 (2008).
100. Hughes, S.W. *et al.* Synchronized oscillations at alpha and theta frequencies in the lateral geniculate nucleus. *Neuron* **42**, 253–268 (2004).
101. Karamah, F.N., Dahleh, M.A., Brown, E.N. & Massaquoi, S.G. Modeling the contribution of lamina 5 neuronal and network dynamics to low frequency EEG phenomena. *Biol. Cybern.* **95**, 289–310 (2006).
102. Castro-Alamancos, M.A. The motor cortex: a network tuned to 7–14 Hz. *Front. Neural Circuits* **7**, 21 (2013).
103. Castro-Alamancos, M.A., Rigas, P. & Tawara-Hirata, Y. Resonance (approximately 10 Hz) of excitatory networks in motor cortex: effects of voltage-dependent ion channel blockers. *J. Physiol. (Lond.)* **578**, 173–191 (2007).
104. Roopun, A.K. *et al.* A beta2-frequency (20–30 Hz) oscillation in nonsynaptic networks of somatosensory cortex. *Proc. Natl. Acad. Sci. USA* **103**, 15646–15650 (2006).
105. Brumberg, J.C., Nowak, L.G. & McCormick, D.A. Ionic mechanisms underlying repetitive high-frequency burst firing in supragranular cortical neurons. *J. Neurosci.* **20**, 4829–4843 (2000).
106. Cunningham, M.O. *et al.* A role for fast rhythmic bursting neurons in cortical gamma oscillations *in vitro*. *Proc. Natl. Acad. Sci. USA* **101**, 7152–7157 (2004).
107. Cardin, J.A., Palmer, L.A. & Contreras, D. Stimulus-dependent gamma (30–50 Hz) oscillations in simple and complex fast rhythmic bursting cells in primary visual cortex. *J. Neurosci.* **25**, 5339–5350 (2005).
108. Wang, X.J. Fast burst firing and short-term synaptic plasticity: a model of neocortical chattering neurons. *Neuroscience* **89**, 347–362 (1999).
109. Hughes, S.W. *et al.* Novel modes of rhythmic burst firing at cognitively-relevant frequencies in thalamocortical neurons. *Brain Res.* **1235**, 12–20 (2008).
110. Whittington, M.A., Traub, R.D. & Jefferys, J.G. Synchronized oscillations in interneuron networks driven by metabotropic glutamate receptor activation. *Nature* **373**, 612–615 (1995).
111. Hormuzdi, S.G. *et al.* Impaired electrical signaling disrupts gamma frequency oscillations in connexin 36-deficient mice. *Neuron* **31**, 487–495 (2001).
112. Xu, H., Jeong, H.Y., Tremblay, R. & Rudy, B. Neocortical somatostatin-expressing GABAergic interneurons disinhibit the thalamorecipient layer 4. *Neuron* **77**, 155–167 (2013).
113. Pfeffer, C.K., Xue, M., He, M., Huang, Z.J. & Scanziani, M. Inhibition of inhibition in visual cortex: the logic of connections between molecularly distinct interneurons. *Nat. Neurosci.* **16**, 1068–1076 (2013).
114. Gibson, J.R., Beierlein, M. & Connors, B.W. Two networks of electrically coupled inhibitory neurons in neocortex. *Nature* **402**, 75–79 (1999).
115. Swadlow, H.A. Fast-spike interneurons and feedforward inhibition in awake sensory neocortex. *Cereb. Cortex* **13**, 25–32 (2003).
116. Hu, H., Ma, Y. & Agmon, A. Submillisecond firing synchrony between different subtypes of cortical interneurons connected chemically but not electrically. *J. Neurosci.* **31**, 3351–3361 (2011).
117. Berger, T.K., Silberberg, G., Perin, R. & Markram, H. Brief bursts self-inhibit and correlate the pyramidal network. *PLoS Biol.* **8**, e1000473 (2010).
118. Flint, A.C. & Connors, B.W. Two types of network oscillations in neocortex mediated by distinct glutamate receptor subtypes and neuronal populations. *J. Neurophysiol.* **75**, 951–957 (1996).
119. Murayama, M. *et al.* Dendritic encoding of sensory stimuli controlled by deep cortical interneurons. *Nature* **457**, 1137–1141 (2009).
120. Carracedo, L.M. *et al.* A neocortical delta rhythm facilitates reciprocal interlaminar interactions via nested theta rhythms. *J. Neurosci.* **33**, 10750–10761 (2013).



Supplementary Figure 1

Thalamo-cortical alpha rhythmic motif.

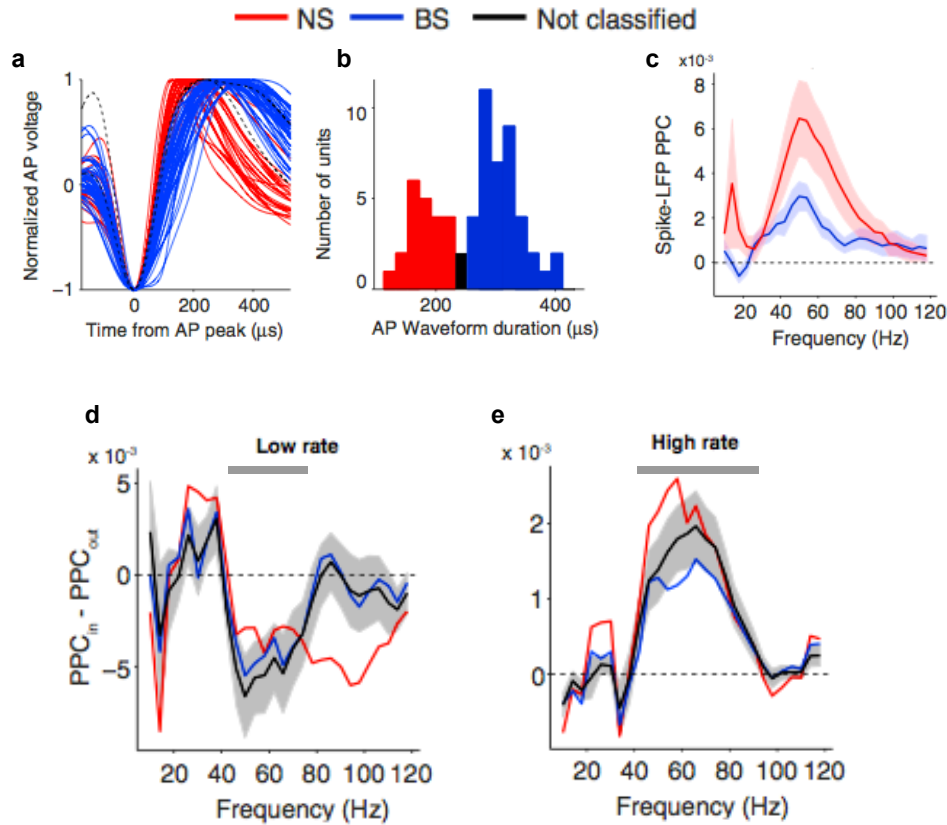
(a) The structural connectivity (top) shows that the alpha rhythmic motif depends on rhythmically bursting, high threshold (HT) cells entraining inhibitory neurons (IN), which in turn impose rhythmic suppression onto relay-mode, regular spiking projection neurons. The bursting frequency of the HT cells depends on intrinsic currents, whereas the synchrony derives from coupling by gap junctions. Depending on whether the IN cells fire single spikes or burst, the relay cells are either in-phase suppressed or anti-phase suppressed. The bottom panels show the cross correlograms illustrating the rhythmic activation of the interneurons (Int) by bursting HT cells (*left*) and the alpha rhythmic inhibition of relay mode cells by an interneurons (*right*). (b) Example activation traces showing the relation of interneuron IPSPs (*bottom*) on relay mode neuron spike generation (middle) and the extracellular recorded filtered LFP (top). The phase-of-firing histogram (*right*) shows that during alpha rhythmic pulsed inhibition relay neuron firing is facilitated particularly in the third quarter of the oscillation cycle. Adapted from Lorincz, M.L., Kekesi, K.A., Juhasz, G., Crunelli, V. & Hughes, S.W. Temporal framing of thalamic relay-mode firing by phasic inhibition during the alpha rhythm. *Neuron* **63**, 683-696, copyright Elsevier (2009).



Supplementary Figure 2

Selective gamma coherence during selective visual processing.

(a) The spatial coverage of ECoG electrode locations (dots) projected on the rendered cortical surface of a macaque brain. Dots indicate the 252 electrodes of a high density ECoG grid. Green and red dots indicate electrodes recording activity over V1 and V4, respectively. 'V1a' and 'V1b' denote two V1 electrode locations recording non-overlapping receptive fields. (b) Stimulus arrangement for the two attention conditions was identical. In one condition attention was directed to the stimulus that activated V4 and the V1a site (stimulus circled in red for illustration purposes). In the other condition attention was directed to the stimulus that activated V4 and the V1b site (stimulus circled in blue for illustration purposes). (c) Spectral power change relative to pre-stimulus baseline (*upper panel*) in V1 in the two attention conditions (red and blue). The bottom panel shows the coherence spectra of the V4 to V1a and V1b (red and blue) when the attended stimulus overlaid V1a (red) and V1b (blue). (d) Illustration of the attention condition (left). Bottom-Up Granger causal influence for the V1a to V4 (red) and the V1b to V4 (blue) connections when the attended stimulus overlaid with V4 and V1a. The rightmost panel shows the respective Top-Down Granger causal influence. (e) Same format as (d) but for the condition with attention on the stimulus that activated the V4 and the V1b recording site. Gray bars in (c,d,e) indicate the frequencies with a significant effect ($p < 0.05$, corrected for multiple comparisons across frequencies, non-parametric randomization across site pairs). Adapted from Bosman, C.A., *et al.* Attentional Stimulus Selection through Selective Synchronization between Monkey Visual Areas. *Neuron* **75**, 875-888, copyright Elsevier (2012).



Supplementary Figure 3

Visual attention and selective 'push-pull' gating in visual cortex at gamma band frequencies mediated by putative interneurons.

(a) Normalized action potential waveforms of single cells recorded in area V4. (b) Distribution of peak-to-trough durations of action potentials across neurons reveals a bimodal distribution that separate narrow spiking from broad spiking cells. (c) Spike-LFP phase locking (measured as pairwise phase consistency) across cells in V4 for narrow and broad spiking cells shows significant gamma band synchronization for NS and BS cells, and significant alpha band synchronization for NS cells. (d,e) Attention (attend inside, PPC_{in} , versus outside, the visual receptive field of the cells, PPC_{out}) decreases gamma band phase locking for NS and BS cells that show low firing rates (d), and increases phase locking for cells with higher firing rates (e). The respective gamma bands are highlighted with grey bars in the top of the panels. This finding suggests a push-pull mechanism of attention that implements the up- and down-modulation of cells' synchronization depending on their overall rate in response to visual stimuli. Low/High firing rate cells were median split. Adapted from Vinck, M., Womelsdorf, T., Buffalo, E.A., Desimone, R. & Fries, P. Attentional modulation of cell-class-specific gamma-band synchronization in awake monkey area v4. *Neuron* **80**, 1077-1089, copyright Elsevier (2013).